

COMPRESSIVE TRACKING OF DOUBLY SELECTIVE CHANNELS IN MULTICARRIER SYSTEMS BASED ON SEQUENTIAL DELAY-DOPPLER SPARSITY

Daniel Eiwen¹, Georg Tauböck², Franz Hlawatsch², and Hans G. Feichtinger¹

¹NuHAG, Faculty of Mathematics, University of Vienna, Austria; daniel.eiwen@univie.ac.at

²Institute of Telecommunications, Vienna University of Technology, Austria; gtauboec@nt.tuwien.ac.at

ABSTRACT

We propose a compressive method for tracking doubly selective channels within multicarrier systems, including OFDM systems. Using the recently introduced concept of modified compressed sensing (MOD-CS), the *sequential* delay-Doppler sparsity of the channel is exploited to improve estimation performance through a recursive estimation mode. The proposed compressive channel tracking algorithm uses a MOD-CS version of OMP with reduced complexity. Simulation results demonstrate substantial performance gains over conventional compressive channel estimation.

Index Terms—OFDM, multicarrier modulation, channel estimation, compressed sensing, sparsity.

1. INTRODUCTION

Many wireless channels tend to be dominated by a relatively small number of clusters of significant paths [1]. This inherent sparsity is exploited by *compressive channel estimation* [2, 3], which makes use of compressed sensing (CS) recovery algorithms like basis pursuit denoising (BPDN) [4] or orthogonal matching pursuit (OMP) [5]. In this paper, we propose a compressive pilot-aided scheme that performs a time-sequential (recursive) estimation, or *tracking*, of doubly selective channels. We consider pulse-shaping multicarrier (MC) systems, which include OFDM systems as a special case.

The proposed compressive channel tracking method is based on the recently introduced concept of *modified compressed sensing* (MOD-CS), which assumes that a part of the support of the signal to be estimated is known *a priori* [6, 7]. In our application of MOD-CS, the prior support information is given by the effective delay-Doppler support estimated during the previous symbol block. This is justified by the fact—demonstrated in this paper—that in typical scenarios, the delay-Doppler support changes only slowly.

A MOD-CS variant of BPDN was proposed in [7]. However, motivated by certain practical advantages of OMP over BPDN [8], we will use a MOD-CS variant of OMP, previously described in [9], which we term the *modified OMP* (MOD-OMP) algorithm. The complexity of MOD-OMP is typically lower than that of OMP.

This paper is organized as follows. The MC system model is recalled in Section 2. In Section 3, we review some MOD-CS fundamentals and state the MOD-OMP algorithm. The MOD-CS-based channel tracking method is presented in Section 4. Section 5 investigates the channel's delay-Doppler sparsity for consecutive symbol blocks. Finally, simulation results demonstrating the achieved performance gains are presented in Section 6.

2. MULTICARRIER SYSTEM MODEL

We assume that Q consecutive symbol blocks of L MC symbols each are transmitted using a pulse-shaping MC system with K subcarriers

This work was supported by the WWTF under grant MA 07-004 (SPORTS) and by the FWF under grants S10602 and S10603 within NFN SISE.

and symbol duration $N \geq K$ [10, 11]. Let $a_{l,k}^{(q)} \in \mathcal{A}$ ($l = 0, \dots, L-1$; $k = 0, \dots, K-1$) denote the complex data symbols of the q th symbol block, with $q \in \{0, \dots, Q-1\}$. Here, \mathcal{A} is a finite symbol alphabet. From the data symbols of all blocks, a discrete-time transmit signal $s[n]$ is computed using a transmit pulse $g[n]$ and converted to a continuous-time transmit signal $s(t)$ through interpolation with filter impulse response $f_1(t)$ and sampling period T_s . Assuming transmission of $s(t)$ over a doubly selective (or doubly dispersive) channel with time-varying impulse response $h(t, \tau)$, the receive signal in the equivalent baseband domain is given by

$$r(t) = \int_{-\infty}^{\infty} h(t, \tau) s(t - \tau) d\tau + z(t), \quad (1)$$

where $z(t)$ is complex noise. At the receiver, $r(t)$ is converted to the discrete-time receive signal $r[n]$ by means of an anti-aliasing filter with impulse response $f_2(t)$ and sampling with period T_s . Subsequently, using a receive pulse $\gamma[n]$, the receiver calculates from $r[n]$ demodulated symbols $r_{l,k}^{(q)}$. The $r_{l,k}^{(q)}$ are then equalized and quantized. For details about the MC transmitter and receiver, see [2, 10, 11].

Assuming a causal channel with maximum delay not larger than $(K-1)T_s$, and neglecting intersymbol/intercarrier interference (which is justified if the channel dispersion is not too strong), one obtains the approximate relation [10]

$$r_{l,k}^{(q)} = H_{l,k}^{(q)} a_{l,k}^{(q)} + z_{l,k}^{(q)}, \quad (2)$$

for $l = 0, \dots, L-1$, $k = 0, \dots, K-1$, and $q = 0, \dots, Q-1$. Here, $z_{l,k}^{(q)}$ is an equivalent noise. Furthermore, the time-frequency channel coefficients $H_{l,k}^{(q)}$ can be written as [2]

$$H_{l,k}^{(q)} = \sum_{m=0}^{K-1} \sum_{i=-L/2}^{L/2-1} F_{m,i}^{(q)} e^{-j2\pi(\frac{km}{K} - \frac{il}{L})} \quad (3)$$

(L is assumed even for mathematical convenience), where

$$F_{m,i}^{(q)} \triangleq \sum_{n=0}^{N-1} S_h^{(q)}[m, i + nL] A_{\gamma,g}^*(m, \frac{i + nL}{LN}). \quad (4)$$

In this expression, $S_h^{(q)}[m, i]$ denotes the *discrete spreading function* [12, 13] for symbol block q (which depends on $f_1(t)$, $h(t, \tau)$, and $f_2(t)$ [2]), and $A_{\gamma,g}(m, \xi) \triangleq \sum_{n=-\infty}^{\infty} \gamma[n] g^*[n-m] e^{-j2\pi\xi n}$ is the *cross-ambiguity function* [14] of $\gamma[n]$ and $g[n]$. The coefficient functions $F_{m,i}^{(q)}$ represent the equivalent channel (2) in terms of a discrete-delay variable m and a discrete-Doppler variable i .

It is worth noting that traditional cyclic-prefix (CP) OFDM is included as a special case, corresponding to a rectangular transmit pulse $g[n]$ that is 1 for $n = 0, \dots, N-1$ and 0 otherwise, and a rectangular receive pulse $\gamma[n]$ that is 1 for $n = N-K, \dots, N-1$ and 0 otherwise ($N-K \geq 0$ is the CP length).

3. MODIFIED COMPRESSED SENSING

A vector is said to be S -sparse if at most S of its entries are nonzero, i.e., if its support \mathcal{S} satisfies $|\mathcal{S}| \leq S$. In a typical CS reconstruction setting, an (approximately) S -sparse vector $\mathbf{x} \in \mathbb{C}^{M_1}$ is to be estimated from a known vector $\mathbf{y} \in \mathbb{C}^{M_2}$, based on the linear model

$$\mathbf{y} = \Phi \mathbf{x} + \mathbf{z}, \quad (5)$$

where $\Phi \in \mathbb{C}^{M_2 \times M_1}$ is a known measurement matrix and $\mathbf{z} \in \mathbb{C}^{M_2}$ is an unknown noise vector. Usually, $M_2 \ll M_1$. Two major approaches to solving this problem are algorithms using convex optimization techniques, like BPDN [4], and greedy algorithms, like OMP [5]. Convex optimization algorithms tend to offer better theoretical performance guarantees, whereas greedy algorithms often yield faster implementations and better results in practice.

In some applications, a part $\mathcal{R} \subseteq \mathcal{S}$ of the support of \mathbf{x} is known *a priori*. An adaptation of BPDN called *modified BPDN* (MOD-BPDN) [7] exploits this information by solving the problem

$$\min_{\mathbf{x}' \in \mathbb{C}^{M_1}} \|\mathbf{x}'|_{\mathcal{R}^c}\|_1 \quad \text{subject to } \|\mathbf{y} - \Phi \mathbf{x}'\|_2 \leq \epsilon,$$

where $\mathbf{x}'|_{\mathcal{R}^c}$ is the restriction of \mathbf{x}' to \mathcal{R}^c , the complement of \mathcal{R} within $\{1, \dots, M_1\}$. MOD-BPDN satisfies desirable performance guarantees [7]. However, in view of certain practical advantages of OMP over BPDN [8], we will here consider a variant of OMP that we call *modified OMP* (MOD-OMP), and which was described in [9]. In an initialization step, the signal is reconstructed on the known support subset \mathcal{R} , and afterwards regular OMP steps are performed on \mathcal{R}^c until a stopping criterion is met. A detailed statement of the MOD-OMP algorithm is as follows.

- **Input:** \mathbf{y} , Φ , \mathcal{R} , S , and target error power level¹ ρ^2 .
- **Initialization:** Solve the least squares (LS) problem

$$\mathbf{x}_0 = \arg \min_{\mathbf{x}': \mathbf{x}'|_{\mathcal{R}^c} = \mathbf{0}} \|\mathbf{y} - \Phi \mathbf{x}'\|_2;$$

calculate the residual $\mathbf{r}_0 = \mathbf{y} - \Phi \mathbf{x}_0$; set $\mathcal{S}_0 = \mathcal{R}$ and $s = 0$.

- **OMP steps:** While $s < S - |\mathcal{R}|$ and $\|\mathbf{r}_s\|_2 > \rho \|\mathbf{y}\|_2$:
 1. increment $s \mapsto s + 1$;
 2. find $n_s = \arg \max_{n \in \mathcal{S}_{s-1}^c} |(\Phi^H \mathbf{r}_{s-1})_n|$; set $\mathcal{S}_s = \mathcal{S}_{s-1} \cup \{n_s\}$;
 3. solve the LS problem $\mathbf{x}_s = \arg \min_{\mathbf{x}': \mathbf{x}'|_{\mathcal{S}_s^c} = \mathbf{0}} \|\mathbf{y} - \Phi \mathbf{x}'\|_2$;
 4. calculate the new residual $\mathbf{r}_s = \mathbf{y} - \Phi \mathbf{x}_s$.
- **Output:** Signal estimate $\hat{\mathbf{x}} = \mathbf{x}_s$.

By an extension of the analysis for OMP in [15], performance guarantees for MOD-OMP in terms of the restricted isometry constant [8, 15, 16] can be shown (omitted here because of limited space; see also [9]). Conventional CS—i.e., no prior partial information about the signal support—corresponds to $\mathcal{R} = \emptyset$; hence, both MOD-BPDN and MOD-OMP coincide with their CS counterparts in this case. As \mathcal{R} approaches \mathcal{S} , fewer OMP steps are required, and thus the computational complexity of MOD-OMP is reduced. It follows that MOD-OMP has a lower complexity than OMP.

If the prior partial-support information \mathcal{R} is only approximate, the initialization of MOD-OMP can be modified as follows. Let $\tilde{\mathbf{x}} \triangleq \arg \min_{\mathbf{x}': \mathbf{x}'|_{\mathcal{R}^c} = \mathbf{0}} \|\mathbf{y} - \Phi \mathbf{x}'\|_2$, and define the subset $\tilde{\mathcal{R}} \subseteq \mathcal{R}$ consisting of those elements of \mathcal{R} for which the magnitudes of the en-

¹If S is exactly known, we use $\rho^2 = 0$. If S is completely unknown, then $S = M_1$ (or, S large enough) is a reasonable choice.

tries of $\tilde{\mathbf{x}}$ are above a given threshold. We then propose to use the subset $\tilde{\mathcal{R}}$ instead of \mathcal{R} for initializing MOD-OMP.

4. COMPRESSIVE CHANNEL TRACKING

We will now describe the proposed channel tracking method. This method generalizes the CS-based estimator of [2]; as a consequence, the following development is initially parallel to that in [2].

For practical (underspread [12, 13]) channels and practical transmit and receive pulses, the coefficients $F_{m,i}^{(q)}$ in (4) are effectively supported in a small rectangular region about the origin, $[0, D-1] \times [-J/2, J/2-1]$, where $D \leq K$, $J \leq L$ is assumed even, and D and J are chosen such that $\Delta K \triangleq K/D$ and $\Delta L \triangleq L/J$ are integers. Because of (3), the channel coefficients $H_{l,k}^{(q)}$ are then determined by their values on the subsampled grid $\mathcal{G} \triangleq \{(l, k) = (\lambda \Delta L, \kappa \Delta K) \mid \lambda = 0, \dots, J-1, \kappa = 0, \dots, D-1\}$, and we have

$$H_{\lambda \Delta L, \kappa \Delta K}^{(q)} = \sum_{m=0}^{D-1} \sum_{i=-J/2}^{J/2-1} F_{m,i}^{(q)} e^{-j2\pi(\frac{\kappa m}{D} - \frac{\lambda i}{J})}. \quad (6)$$

In [2], it has been shown for a simple channel model that the 2D DFT coefficients $F_{m,i}^{(q)}$ (for q fixed) are approximately sparse, with the sparsity level limited by leakage effects. To mitigate these leakage effects and thereby enhance the sparsity, we generalize (6) to an orthonormal 2D basis expansion

$$H_{\lambda \Delta L, \kappa \Delta K}^{(q)} = \sum_{m=0}^{D-1} \sum_{i=-J/2}^{J/2-1} \alpha_{m,i}^{(q)} u_{m,i}[\lambda, \kappa]. \quad (7)$$

A “sparsity-enhancing” construction of the basis $\{u_{m,i}[\lambda, \kappa]\}$ has been proposed in [2]. We assume that the coefficient functions $\alpha_{m,i}^{(q)}$ are approximately S -sparse, with $S \leq JD$. We can rewrite (7) as

$$\mathbf{h}^{(q)} = \mathbf{U} \boldsymbol{\alpha}^{(q)}, \quad (8)$$

where $\mathbf{h}^{(q)} \triangleq \text{vec}_{\lambda, \kappa} \{H_{\lambda \Delta L, \kappa \Delta K}^{(q)}\} \in \mathbb{C}^{JD}$ (i.e., $\mathbf{h}^{(q)} = (h_1^{(q)} \dots h_{JD}^{(q)})^T$ with $h_{\kappa J + \lambda + 1}^{(q)} = H_{\lambda \Delta L, \kappa \Delta K}^{(q)}$); $\mathbf{U} \in \mathbb{C}^{JD \times JD}$ is a unitary matrix whose $((i+J/2)D+m+1)$ th column is given by the vector $\text{vec}_{\lambda, \kappa} \{u_{m,i}[\lambda, \kappa]\}$; and $\boldsymbol{\alpha}^{(q)} \triangleq \text{vec}_{m,i} \{\alpha_{m,i}^{(q)}\} \in \mathbb{C}^{JD}$.

For pilot-aided channel estimation, pilot symbols $a_{l,k}^{(q)} = p_{l,k}^{(q)}$ are transmitted at time-frequency positions $(l, k) \in \mathcal{P}^{(q)}$, where $\mathcal{P}^{(q)} \subset \mathcal{G}$. The receiver then calculates channel estimates $\hat{H}_{l,k}^{(q)} \triangleq r_{l,k}^{(q)} / p_{l,k}^{(q)} = H_{l,k}^{(q)} + z_{l,k}^{(q)} / p_{l,k}^{(q)}$ (cf. (2)) at the pilot positions $(l, k) \in \mathcal{P}^{(q)}$. Reducing (8) to these pilot positions yields $\tilde{\mathbf{h}}^{(q)} = \mathbf{U}^{(q)} \boldsymbol{\alpha}^{(q)}$, which involves the corresponding length- $|\mathcal{P}^{(q)}|$ subvector $\tilde{\mathbf{h}}^{(q)}$ of $\mathbf{h}^{(q)}$ and the corresponding $|\mathcal{P}^{(q)}| \times JD$ submatrix $\mathbf{U}^{(q)}$ of \mathbf{U} . Scaling the columns of $\mathbf{U}^{(q)}$ so that they have unit ℓ_2 -norm,² i.e., $\tilde{\Phi}^{(q)} \triangleq \mathbf{U}^{(q)} \mathbf{D}^{(q)}$ with a nonsingular diagonal matrix $\mathbf{D}^{(q)}$, yields $\tilde{\mathbf{h}}^{(q)} = \tilde{\Phi}^{(q)} \mathbf{x}^{(q)}$, where $\mathbf{x}^{(q)} \triangleq \mathbf{D}^{(q)-1} \boldsymbol{\alpha}^{(q)}$ equals $\boldsymbol{\alpha}^{(q)}$ up to known scaling factors. Let $\mathbf{y}^{(q)}$ denote the pilot-based estimate of $\tilde{\mathbf{h}}^{(q)}$. Using $\hat{H}_{l,k}^{(q)} = H_{l,k}^{(q)} + z_{l,k}^{(q)} / p_{l,k}^{(q)}$, we obtain

$$\mathbf{y}^{(q)} = \tilde{\mathbf{h}}^{(q)} + \mathbf{z}^{(q)} = \tilde{\Phi}^{(q)} \mathbf{x}^{(q)} + \mathbf{z}^{(q)}, \quad (9)$$

where $\mathbf{z}^{(q)}$ is the vector with entries $z_{l,k}^{(q)} / p_{l,k}^{(q)} \big|_{(l,k) \in \mathcal{P}^{(q)}}$. This equation is of the form (5), with dimensions $M_2 \triangleq |\mathcal{P}^{(q)}|$ and $M_1 = JD$.

²This scaling is motivated by CS theory [2, 16].

In practice, $M_2 \ll JD$. Since the expansion coefficients $\alpha_{m,i}^{(q)}$ were assumed to be sparse, the vector $\mathbf{x}^{(q)}$ is sparse, too. Therefore, one could use a CS recovery algorithm like BPDN or OMP to obtain an estimate of $\mathbf{x}^{(q)}$ from $\mathbf{y}^{(q)}$ based on (9). This would correspond to conventional compressive channel estimation as in [2].

Here, we propose a different approach. As shown in Section 5, the supports of two consecutive DFT coefficient functions $F_{m,i}^{(q)}$ and $F_{m,i}^{(q+1)}$ overlap to an extent that depends on the spatial geometry and the velocities of transmitter, receiver, and scatterers. Thus, if the DFT basis $\{u_{m,i}[\lambda, \kappa] = \frac{1}{\sqrt{JD}} e^{-j2\pi(\frac{\lambda m}{D} - \frac{\lambda \kappa}{J})}\}$ is used, $\mathbf{x}^{(q)}$ and $\mathbf{x}^{(q+1)}$ have overlapping supports. Simulation studies demonstrate that this is still true if $\{u_{m,i}[\lambda, \kappa]\}$ is optimized as described in [2].

This motivates the following channel tracking method, which we describe for a general basis $\{u_{m,i}[\lambda, \kappa]\}$. For the first symbol block ($q=0$), we use conventional compressive channel estimation as discussed above to obtain an estimate $\hat{\mathbf{x}}^{(0)}$ of $\mathbf{x}^{(0)}$. After scaling $\hat{\mathbf{x}}^{(0)}$ with $\mathbf{D}^{(0)}$, we obtain an estimate $\hat{\boldsymbol{\alpha}}^{(0)} = \mathbf{D}^{(0)} \hat{\mathbf{x}}^{(0)}$ of $\boldsymbol{\alpha}^{(0)}$ and, further, an estimate of the subsampled channel coefficients $H_{\lambda \Delta L, \kappa \Delta K}^{(0)}$ according to (7). Finally, inverting (6) to obtain estimated DFT coefficients $\hat{F}_{m,i}^{(0)}$ and using (3) gives estimates of all $H_{l,k}^{(0)}$.

For the remaining blocks, we use a MOD-CS recovery algorithm in a sequential (recursive) manner. Suppose we already calculated an estimate $\hat{\mathbf{x}}^{(q)}$ of $\mathbf{x}^{(q)}$ for some $q \in \{0, \dots, Q-2\}$. Then, we obtain an estimate $\hat{\mathbf{x}}^{(q+1)}$ of $\mathbf{x}^{(q+1)}$ by means of MOD-BPDN or MOD-OMP, using for the prior support $\mathcal{R}^{(q)}$ that part of the support of $\hat{\mathbf{x}}^{(q)}$ that is expected to best match the support of $\mathbf{x}^{(q+1)}$. Because we do not know $\mathbf{x}^{(q+1)}$, we define $\mathcal{R}^{(q)}$ as the set of the indices of the $|\mathcal{R}^{(q)}|$ entries of $\hat{\mathbf{x}}^{(q)}$ with largest magnitudes, for a prescribed cardinality $|\mathcal{R}^{(q)}|$, or, alternatively, as the set of the indices of all entries of $\hat{\mathbf{x}}^{(q)}$ whose magnitudes are above a prescribed threshold $\gamma > 0$. Then, we proceed similarly as explained further above for $\hat{\mathbf{x}}^{(0)}$: we scale the estimate $\hat{\mathbf{x}}^{(q+1)}$ with $\mathbf{D}^{(q+1)}$, calculate estimates of $H_{\lambda \Delta L, \kappa \Delta K}^{(q+1)}$ according to (7), invert (6) to obtain $\hat{F}_{m,i}^{(q+1)}$, and finally use (3) to get estimates of all $H_{l,k}^{(q+1)}$. We note that conventional compressive channel estimation is reobtained if $\mathcal{R}^{(q)} = \emptyset$ for all $q = 0, \dots, Q-2$.

For consistency with the standard construction of the measurement matrix $\Phi^{(q)}$ [16], the pilot positions $\mathcal{P}^{(q)}$ are chosen uniformly at random from the subsampled grid \mathcal{G} . For $|\mathcal{P}^{(q)}|$ sufficiently large, this implies desirable performance guarantees, cf. [2] and Section 3.

5. SEQUENTIAL DELAY-DOPPLER SPARSITY

In this section, extending our analysis in [2, 17], we study the “sequential sparsity” of the delay-Doppler channel coefficients $F_{m,i}^{(q)}$. We assume that for each symbol block $q \in \{0, \dots, Q-1\}$, the channel comprises P propagation paths corresponding to the same P specular scatterers with q -dependent time delays $\tau_p^{(q)}$ and Doppler frequency shifts $\nu_p^{(q)}$ ($p = 1, \dots, P$). We also assume that $\tau_p^{(q)}$ and $\nu_p^{(q)}$ remain constant over the duration T_b of the q th symbol block ($T_b \approx T_s NL$, see [2]). We note that these assumptions are only made for analyzing the sequential sparsity of the $F_{m,i}^{(q)}$; they are not needed for our channel tracking method. For this channel model, the impulse response for $t \in [qT_b, (q+1)T_b)$ can be written as

$$h^{(q)}(t, \tau) = \sum_{p=1}^P \eta_p \delta(\tau - \tau_p^{(q)}) e^{j2\pi\nu_p^{(q)}t},$$

where η_p characterizes the complex attenuation of the p th propagation path and $\delta(\cdot)$ is the Dirac delta. Because η_p does not depend on

q , paths are not allowed to vanish or reappear for different blocks. (However, small variations of η_p with q do not invalidate our analysis.) The spreading function for block q (cf. (4)) then becomes [2]

$$S_h^{(q)}[m, i] = \sum_{p=1}^P \eta_p e^{j\pi(\nu_p^{(q)} T_s - \frac{i}{NL})(NL-1)} \Lambda_p^{(q)}[m, i], \quad (10)$$

with the *shifted leakage kernels*

$$\Lambda_p^{(q)}[m, i] \triangleq \phi_p^{(q)}(m - \tau_p^{(q)}/T_s) \psi(i - \nu_p^{(q)} T_s NL),$$

where $\phi_p^{(q)}(x) \triangleq \int_{-\infty}^{\infty} e^{-j2\pi\nu_p^{(q)}t} f_1(T_s x - t) f_2(t) dt$ and $\psi(x) \triangleq \sin(\pi x)/[NL \sin(\pi x/NL)]$. The p th leakage kernel $\Lambda_p^{(q)}[m, i]$ is effectively supported in a rectangular region of size $\Delta m \times \Delta i$, with some Δm and Δi , that is centered about the delay-Doppler point $\zeta_p^{(q)} \triangleq (\tau_p^{(q)}/T_s, \nu_p^{(q)} T_s NL)$ [2]. Therefore, each $\Lambda_p^{(q)}[m, i]$ can be considered approximately S_Λ -sparse, where $S_\Lambda = \Delta m \Delta i$.

For a given block q , let $\mathbf{w}_{T,p}^{(q)}$ be the vector connecting a given scatterer p with the transmitter, and $\mathbf{w}_{R,p}^{(q)}$ the vector connecting that scatterer with the receiver. Furthermore, let $\mathbf{v}_{T,p}^{(q)}$ and $\mathbf{v}_{R,p}^{(q)}$ be the velocity vectors of, respectively, the transmitter and the receiver relative to scatterer p , and let $w_{T,p}^{(q)} \triangleq \|\mathbf{w}_{T,p}^{(q)}\|_2$, $w_{R,p}^{(q)} \triangleq \|\mathbf{w}_{R,p}^{(q)}\|_2$, $v_{T,p}^{(q)} \triangleq \|\mathbf{v}_{T,p}^{(q)}\|_2$, and $v_{R,p}^{(q)} \triangleq \|\mathbf{v}_{R,p}^{(q)}\|_2$. The time delay for scatterer p is then given by $\tau_p^{(q)} = (w_{T,p}^{(q)} + w_{R,p}^{(q)})/c$, where c is the speed of light, and the Doppler shift for scatterer p is $\nu_p^{(q)} = \frac{f_0}{c} (\mathbf{v}_{T,p}^{(q)T} \mathbf{w}_{T,p}^{(q)} / w_{T,p}^{(q)} + \mathbf{v}_{R,p}^{(q)T} \mathbf{w}_{R,p}^{(q)} / w_{R,p}^{(q)})$, where f_0 denotes the carrier frequency.

For two consecutive blocks q and $q+1$, we have $\mathbf{w}_{T,p}^{(q+1)} \approx \mathbf{w}_{T,p}^{(q)} + T_b \mathbf{v}_{T,p}^{(q)}$ and $\mathbf{w}_{R,p}^{(q+1)} \approx \mathbf{w}_{R,p}^{(q)} + T_b \mathbf{v}_{R,p}^{(q)}$. Therefore, the time delay difference $\Delta\tau_p^{(q)} \triangleq |\tau_p^{(q+1)} - \tau_p^{(q)}|$ can be (approximately) bounded as $\Delta\tau_p^{(q)} \leq \tau_{B,p}^{(q)}$, with

$$\tau_{B,p}^{(q)} = \frac{T_b (v_{T,p}^{(q)} + v_{R,p}^{(q)})}{c}. \quad (11)$$

Moreover, using the triangle and Cauchy-Schwarz inequalities, the Doppler shift difference $\Delta\nu_p^{(q)} \triangleq |\nu_p^{(q+1)} - \nu_p^{(q)}|$ can be shown to satisfy $\Delta\nu_p^{(q)} \leq \nu_{B,p}^{(q)}$, with

$$\nu_{B,p}^{(q)} = \frac{f_0}{c} \left(\Delta v_{T,p}^{(q)} + 2v_{T,p}^{(q+1)} \frac{\Delta w_{T,p}^{(q)}}{w_{T,p}^{(q)}} + \Delta v_{R,p}^{(q)} + 2v_{R,p}^{(q+1)} \frac{\Delta w_{R,p}^{(q)}}{w_{R,p}^{(q)}} \right), \quad (12)$$

where $\Delta v_{T,p}^{(q)} \triangleq \|\mathbf{v}_{T,p}^{(q+1)} - \mathbf{v}_{T,p}^{(q)}\|_2$, $\Delta v_{R,p}^{(q)} \triangleq \|\mathbf{v}_{R,p}^{(q+1)} - \mathbf{v}_{R,p}^{(q)}\|_2$, $\Delta w_{T,p}^{(q)} \triangleq \|\mathbf{w}_{T,p}^{(q+1)} - \mathbf{w}_{T,p}^{(q)}\|_2 \approx T_b v_{T,p}^{(q)}$, and $\Delta w_{R,p}^{(q)} \triangleq \|\mathbf{w}_{R,p}^{(q+1)} - \mathbf{w}_{R,p}^{(q)}\|_2 \approx T_b v_{R,p}^{(q)}$.

We now recall that the leakage kernel for path p , $\Lambda_p^{(q)}[m, i]$, is centered about the delay-Doppler point $\zeta_p^{(q)} = (\tau_p^{(q)}/T_s, \nu_p^{(q)} T_s NL)$. The above bounds on $\Delta\tau_p^{(q)}$ and $\Delta\nu_p^{(q)}$ show that the center points $\zeta_p^{(q)}$ and $\zeta_p^{(q+1)}$ of the leakage kernels for two consecutive blocks q and $q+1$ differ at most by $\Delta m_{B,p}^{(q)} \triangleq \lceil \tau_{B,p}^{(q)}/T_s \rceil$ in the m direction and by $\Delta i_{B,p}^{(q)} \triangleq \lceil \nu_{B,p}^{(q)} T_s NL \rceil$ in the i direction. For practical velocities $v_{T,p}^{(q)}$ and $v_{R,p}^{(q)}$ and parameters N and L , it follows from (11) with $T_b \approx T_s NL$ that $\Delta m_{B,p}^{(q)}$ will be small. Furthermore, if

the velocities do not change too quickly, i.e., if $\Delta v_{T,p}^{(q)}$ and $\Delta v_{R,p}^{(q)}$ are small, and if the relative distance variations $\Delta w_{T,p}^{(q)}/w_{T,p}^{(q)}$ and $\Delta w_{R,p}^{(q)}/w_{R,p}^{(q)}$ are not too large (this is typically true in practice), it follows from (12) that $\Delta i_{B,p}^{(q)}$ will be small. Therefore, the supports of $\Lambda_p^{(q)}[m, i]$ and $\Lambda_p^{(q+1)}[m, i]$, and consequently (see (10)) of $S_h^{(q)}[m, i]$ and $S_h^{(q+1)}[m, i]$, and in turn (see (4)) of $F_{m,i}^{(q)}$ and $F_{m,i}^{(q+1)}$, have a large overlap. This demonstrates the sequential delay-Doppler sparsity of practical channels and justifies the basic rationale underlying our compressive channel tracking method.

6. SIMULATION RESULTS

We simulated a CP-OFDM system with $K = 512$ subcarriers, CP length $N-K = 128$, QPSK symbols, carrier frequency $f_0 = 5$ GHz, and bandwidth $B = 1/T_s = 5$ MHz. The system employed Gray labeling, a rate-1/2 convolutional code, and 32×16 row-column interleaving. The interpolation/anti-aliasing filters $f_1(t) = f_2(t)$ were root-raised-cosine filters with roll-off factor 1/4.

We used the channel simulation tool `IlmProp` [18] to generate a doubly selective channel during $Q = 10$ blocks of $L = 32$ OFDM symbols each. For each simulation run, the transmitter and receiver were separated by approximately 1500 m, and 7 clusters of 10 specular scatterers each were randomly distributed between them. Of these, 3 clusters surrounded the receiver within a distance of up to 100 m. Scatterers and receiver were assigned random velocity and acceleration vectors with uniformly distributed directions, velocities of up to 50 m/s, and accelerations of up to 7 m/s².

The discrete version of the noise $z(t)$ in (1) was complex white Gaussian, with its variance σ_z^2 adjusted to achieve a prescribed receive signal-to-noise ratio (SNR). The SNR is defined as the mean receive signal power averaged over one block of length NL , divided by σ_z^2 . The pilot set was identical for all OFDM blocks, i.e., $\mathcal{P}^{(q)} \equiv \mathcal{P}$, and chosen randomly from the subsampled grid \mathcal{G} (the grid spacings were $\Delta L = 1$ and $\Delta K = 4$). We used $|\mathcal{P}| = 1024$ pilots, corresponding to 6.25% of all symbols.

We compared our channel tracking method using MOD-OMP with conventional compressive channel estimation using OMP [2]. For both methods, the 2D DFT basis and an optimized basis (designed as in [2]) were used. For MOD-OMP, $\mathcal{R}^{(q)}$ was chosen as the 95% of the support of $\hat{\mathbf{x}}^{(q)}$ corresponding to the largest-magnitude entries of $\hat{\mathbf{x}}^{(q)}$. In Fig. 1, we show the normalized mean-square error (MSE) of channel tracking/estimation and the bit error rate (BER) as a function of the SNR. It can be seen that compressive channel tracking outperforms conventional compressive channel estimation both for the 2D DFT basis and for the optimized basis. Additionally, since $|\mathcal{R}^{(q)}|$ is quite large, the computational complexity is reduced substantially.

7. CONCLUSION

Based on the recently introduced concept of modified compressed sensing, we extended the compressive estimation of doubly selective channels to a sequential tracking operation where channel estimates are recursively updated. Our compressive channel tracker uses a modified version of the OMP recovery algorithm that exploits partial support information and has a lower complexity than the classic OMP algorithm. Simulation results demonstrated substantial performance gains over conventional compressive channel estimation.

8. REFERENCES

[1] V. Raghavan, G. Hariharan, and A. M. Sayeed, "Capacity of sparse multipath channels in the ultra-wideband regime," *IEEE J. Sel. Topics Signal Process.*, vol. 1, pp. 357–371, Oct. 2007.

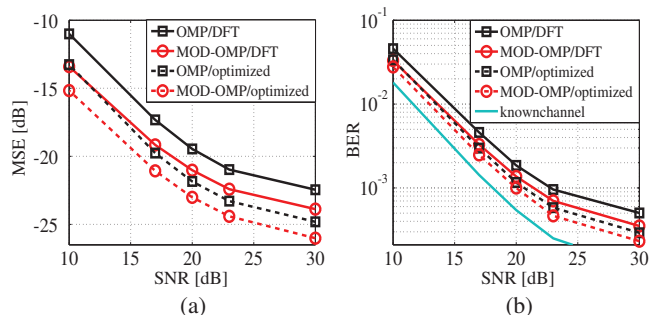


Fig. 1. Performance of the proposed compressive channel tracking method and of conventional compressive channel estimation: (a) MSE versus SNR, (b) BER versus SNR.

[2] G. Tauböck, F. Hlawatsch, D. Eiwien, and H. Rauhut, "Compressive estimation of doubly selective channels in multicarrier systems: Leakage effects and sparsity-enhancing processing," *IEEE J. Sel. Topics Signal Process.*, vol. 4, pp. 255–271, April 2010.

[3] W. U. Bajwa, J. Haupt, A. M. Sayeed, and R. Nowak, "Compressed channel sensing: A new approach to estimating sparse multipath channels," *Proc. IEEE*, vol. 98, pp. 1058–1076, June 2010.

[4] E. Candès, "The restricted isometry property and its implications for compressed sensing," *Comptes Rendus Mathématique*, vol. 346, pp. 589–592, May 2008.

[5] J. A. Tropp, "Greed is good: Algorithmic results for sparse approximation," *IEEE Trans. Inf. Theory*, vol. 50, pp. 2231–2242, Oct. 2004.

[6] N. Vaswani and W. Lu, "Modified-CS: Modifying compressive sensing for problems with partially known support," *IEEE Trans. Signal Process.*, vol. 58, pp. 4595–4607, Sept. 2010.

[7] W. Lu and N. Vaswani, "Modified basis pursuit denoising (modified-BPDN) for noisy compressive sensing with partially known support," in *Proc. IEEE ICASSP-2010*, Dallas, TX, pp. 3926–3929, March 2010.

[8] H. Rauhut, "Stability results for random sampling of sparse trigonometric polynomials," *IEEE Trans. Inf. Theory*, vol. 54, pp. 5661–5670, Dec. 2008.

[9] T. Zhang, "Sparse recovery with orthogonal matching pursuit under RIP." Available online: arXiv:1005.2249v1 [cs.IT], May 2010.

[10] W. Kozek and A. F. Molisch, "Nonorthogonal pulseshapes for multicarrier communications in doubly dispersive channels," *IEEE J. Sel. Areas Comm.*, vol. 16, pp. 1579–1589, Oct. 1998.

[11] G. Matz, D. Schaffhuber, K. Gröchenig, M. Hartmann, and F. Hlawatsch, "Analysis, optimization, and implementation of low-interference wireless multicarrier systems," *IEEE Trans. Wireless Comm.*, vol. 6, pp. 1921–1931, May 2007.

[12] P. A. Bello, "Characterization of randomly time-variant linear channels," *IEEE Trans. Comm. Syst.*, vol. 11, pp. 360–393, Dec. 1963.

[13] G. Matz and F. Hlawatsch, "Fundamentals of time-varying communication channels," in *Wireless Communications over Rapidly Time-Varying Channels* (F. Hlawatsch and G. Matz, eds.), Academic Press, 2011.

[14] P. Flandrin, *Time-Frequency/Time-Scale Analysis*. San Diego, CA: Academic Press, 1999.

[15] M. Davenport and M. Wakin, "Analysis of orthogonal matching pursuit using the restricted isometry property," *IEEE Trans. Inf. Theory*, vol. 56, pp. 4395–4401, Sept. 2010.

[16] M. Rudelson and R. Vershynin, "Sparse reconstruction by convex relaxation: Fourier and Gaussian measurements," in *Proc. 40th Annu. Conf. Inform. Sci. Syst. (CISS'06)*, Princeton, NJ, pp. 207–212, March 2006.

[17] D. Eiwien, G. Tauböck, F. Hlawatsch, H. Rauhut, and N. Czink, "Multichannel-compressive estimation of doubly selective channels in MIMO-OFDM systems: Exploiting and enhancing joint sparsity," in *Proc. IEEE ICASSP-2010*, Dallas, TX, pp. 3082–3085, March 2010.

[18] G. Del Galdo and M. Haardt, "IlmProp: A flexible geometry-based simulation environment for multiuser MIMO communications," in *COST 273 Temporary Document, No. TD(03)188*, Prague, Czech Republic, Sept. 2003.